QUANTIFICATION BY MODELING AND MEASUREMENT OF AIRCRAFT CONTRIBUTION TO AIR POLLUTION IN AIRPORT AREA

Mihaiella CREȚU[1], Tănase DOBRE[2], Victoria TELEABA[3], Luminița DRĂGĂȘANU[4]

Primary pollutants emitted by aircraft engines during the LTO cycle affect air quality both within and neighborhood the airport. These pollutants are subject to wind transport and chemical processes in the atmosphere and have adverse effects on human health and, in general, on the environment.

Referring to an airport, it shown that is important to estimate the contribution of aircraft to air pollution.

The paper presents the results obtained by modeling NO_x pollutant dispersion emitted by aircrafts engines during take-off procedure and monitoring campaign to check the results obtained by modeling.

Keywords: aircraft emissions, nitrogen oxides NO_x, LTO-cycle, measurement, modeling, pollutant dispersion, air quality

1. Introduction

High concentrations of air pollutants result during take-off and landing procedures of aircrafts, as well as their ground movement (LTO cycle), that have adverse effects on human health and the environment, causing air pollution in and neighborhood airports.

Aircraft engines emit carbon dioxide (CO_2), water vapors, nitrogen oxides (NO_x), carbon monoxide (CO), sulfur oxides (SO_x), unburned hydrocarbons (COV), fine primary particles (PM2.5) and traces of other dangerous pollutants.

Due to complex photochemical processes associated with ozone formation, depending on local quantities of NO_x, COV and ozone catalysts (OH and HO_2 radicals), NO_x emissions lead to the formation of tropospheric ozone.

[1] Eng., COMOTI - Romanian R&D Institute for Gas Turbines, Bucharest, Romania, e-mail: mihaela.cretu@comoti.ro

[2] Professor, Chemical Engineering Department, University POLITEHNICA of Bucharest, Romania, e-mail: tghdobre@gmail.com

[3] Eng., COMOTI - Romanian R&D Institute for Gas Turbines, Bucharest, Romania, e-mail: victoria.teleaba@comoti.ro

[4] Eng., COMOTI - Romanian R&D Institute for Gas Turbines, Bucharest, Romania, e-mail: luminita.dragasanu@comoti.ro

The increasing of NO_x emissions rise ozone concentrations in suburban and rural areas, if there are many sources of COV [1]. Nitrogen oxide is a generic term including nitrogen dioxide (NO_2) and nitrogen oxide (NO). Because NO is rapidly oxidized to NO_2, emissions are expressed in terms of nitrogen dioxide (NO_2) equivalent. Nitrogen oxides are formed during the combustion of fuels, especially at high temperatures [2].

The increasing of air traffic could result in overflowing of NO_2 limit values provided by the national/European regulations and designed to maintain air quality parameters. In the European Union, ambient standards for NO_2 have recently been tightened, and along with the World Health Organization (WHO), guidelines of a 40 μg/m^3 annual average and a 200 μg/m^3 for maximum one hour were established [3] [4].

Considering all these aspects, during last decade a lot of studies are also focusing on the aircraft emissions impact on local and regional air quality in the vicinity of airport. The basic objects of attention are nitrogen oxide and fine particle emissions from aircraft engine emissions as initiators of photochemical smog and regional haze, which directly impact human health [5] [6].

This paper presents the results obtained by dispersion modeling for NO_x pollutant emitted by aircraft engines during takeoff operation, and the values obtained by monitoring. These experimental investigations are required to verify the results obtained by modeling.

2. Theoretical aspects of NO_x pollutant dispersion modeling

Gaussian puff model was proposed to be used for NO_x pollutant dispersion modeling in order to determine its concentration at receptor location, after each departure of an aircraft. The basic relation of this model [7] is concentrated by relation (1), which give the pollutant concentration in a puff at receptor coordinates.

$$c = \frac{\Delta M}{(2\pi)^{3/2}\sigma_x\sigma_y\sigma_z}\exp\left[-\frac{1}{2}\left(\frac{x_p - x_r}{\sigma_x}\right)^2\right]\exp\left[-\frac{1}{2}\left(\frac{y_p - y_r}{\sigma_y}\right)^2\right]$$
$$\left\{\exp\left[-\frac{1}{2}\left(\frac{z_p - z_r}{\sigma_z}\right)^2\right] + \exp\left[-\frac{1}{2}\left(\frac{z_p + z_r}{\sigma_z}\right)\right] + \exp\left[-\frac{1}{2}\left(\frac{2H_m - z_p - z_r}{\sigma_z}\right)^2\right]\right\} \quad (1)$$

Here c is the pollutant concentration at the receptor (μg/m^3); ΔM represent the mass pollutant in puff (g); x_p, y_p, z_p are center coordinates of a puff (m); x_r, y_r, z_r show the coordinates of receptor position (m); H_m give the mixing height (m); $\sigma_x, \sigma_y, \sigma_z$ are the pollutant dispersion parameter for x, y and respectively z

direction. Gaussian dispersion model used in the paper may provide satisfactory predictions on a distance up to 10 km.

The following hypothesis were assumed when the above field of pollutant concentration has been developed: (1) pollutants are considered non reactive; (2) abscissa *x* of the coordinate system is focused on wind direction; (3) atmospheric factors are constant over time; (4) the turbulent diffusion coefficient for x ,y and z axes have a constant value; (5) the puff movement is made on wind direction without any resistance; (6) atmospheric stability correspond to D class; (7) the aircraft acceleration during take-off is constant. Some considerations, necessary to achieve the modeling are defined hereinafter. They are related with the computation of variables H_m, $\sigma_x, \sigma_y, \sigma_z$ and ΔM, which are contained in Gaussian puff model (1). For that puff rise, puff advection due to wind, atmospheric turbulence and puff rice induced by this turbulence are considered as computable elements in Gaussian model.

a) Puff Rise. The relations (2) and (3) are used to determine the gradual rise of the puff, because of exhausted gases flow [8]. Here ΔH is the puff rise height after x distance traveled (m), F represent the buoyancy flux (m^4/s^3), x shows the horizontal distance traveled by the puff (m), u_z give the wind speed at the height of the centre of a puff (m/s), g is the gravitational acceleration (9,81 m/s^2), v_e introduce the velocity of exhaust gases (m/s), d is the diameter of exhaust point (m), T_e and T_a are temperature of exhaust gases respectively ambient air temperature (K)

$$\Delta H = 1{,}6F^{1/3}x^{2/3}/u_z \tag{2}$$

$$F = gv_e d^2(T_e - T_a)/4T_e \tag{3}$$

The speed of gas and air jet, exhausted from modern turbofan engines (v_e in km/h) depends [9] on aircraft traction force (F_n in KN), mass flow rate at engine exit (G_m in Kg/s) and aircraft speed (v_a in km/h), resulting from relation (4).

$$F_n = G_m(v_e - v_a) \tag{4}$$

The state of puff final rise, characterized by ΔH_f, is modeled using empirical equations based on atmospheric stability. For the *unstable and neutral conditions (stability classes A-D),* equations 5 or 6 are used to determine final buoyancy rise depending of the value of F.

$$\Delta H_f = 21{,}425F^{3/4}/u_z \qquad \text{for } F < 55 \tag{5}$$

$$\Delta H_f = 38{,}71F^{3/5}/u_z \qquad \text{for F} \geq 55 \tag{6}$$

For *stable conditions (stability classes E and F)* first is determined an intermediate variable *s* (in s^{-2}), named stability parameter. Now the relations (8) or

(9) are used for ΔH_f computation. In the mentioned relations $d\theta/dz$ is the temperature gradient respect to height (K/m).

$$s = g(d\theta/dz)/T_a \tag{7}$$

$$\Delta H_f = 2{,}6((F/(u_z s))^{1/3} \tag{8}$$

$$\Delta H_f = 4F^{1/4} s^{-3/8} \tag{9}$$

The lower of these two values, obtained from (8) and (9), represents the final buoyancy rise under stabile conditions

b) Puff advection due to wind. The puff is pushed in the x and y direction by the corresponding components of the wind. The relations (10) and (11), where w_x, w_y is the horizontal components of wind speed (m/s), u_z represent the wind speed at the height of the center of a puff (m/s) and θ shows the wind direction (degrees), give the wind action velocities:

$$w_x = -u_z \sin(\theta) \tag{10}$$

$$w_y = -u_z \cos(\theta) \tag{11}$$

The wind speed (u_z) at the height (z), reported to the puff center, is determined by using a power law equation respect to reference height (z_r, which is usually 10 m, and where the wind velocity is u_r), as it is indicated by equation (12). It shows that the power *p* is dependent on the atmospheric stability class and also on sol surface roughness [10].

$$u_z = u_r(z/z_r)^p \tag{12}$$

c) Atmospheric turbulence. The atmospheric turbulence is considered using the Pasquill-Gilford axis dispersion parameters [11]. Equations (13) and (14), where a, b, c, d are coefficients based on stability classes and where r is the puff cumulative horizontal traveled distance (km), are used to determine these parameters.

$$\sigma_{xt} = \sigma_{yt} = \{1000 \cdot r \cdot \tan[a - b \cdot \ln(r)]\}/2.15 \tag{13}$$

$$\sigma_{zt} = cr^d \tag{14}$$

d) Rice induced turbulence. When the puff rises, it entrains the surrounding air through shearing and/ or by forming of circular eddies. Air entrainment causes the puff increasing and the concentration decreasing. The induced dispersion, which increase with ΔH, is modeled as a function of atmospheric rise [12], as it follows:

$$\sigma_{xr} = \sigma_{yr} = \sigma_{zr} = \Delta H/3{,}5 \tag{15}$$

The dispersion coefficients σ_x, σ_y, and σ_z, from Gaussian puff model, are calculated taking into account the both turbulence (atmospheric and due to puff rice). It uses the relations (16)-(18).

$$\sigma_x = (\sigma_{xt}^2 + \sigma_{xr}^2)^{1/2} \tag{16}$$

$$\sigma_y = (\sigma_{yt}^2 + \sigma_{yr}^2)^{1/2} \tag{17}$$

$$\sigma_z = (\sigma_{zt}^2 + \sigma_{zr}^2)^{1/2} \tag{18}$$

e) Calculation of the NO_x Emission Value for an Aircraft. The NO_x quantity contained by all puffs within the LTO cycle of one aircraft depend only aircraft engines. It is calculated by using the ICAO measured values for LTO-modes of the individual engine [13]. The relation (19) details this calculus. Here n_e is the number of engines fitted to the aircraft, τ_k represent the time period of sequence *k* from LTO cycle - (min), F_k give the fuel flow rate for *k* sequence of LTO cycle - (kg/s), $i_{NOx,k}$ shows the NO_x emission index per *k* sequence - (gNO_x/kg fuel)

$$m_{NO_x aircraft} = n_e * \sum_k \left(60 * \tau_k * F_k * i_{NOx,k} \div 1000\right) \tag{19}$$

3. Experimental activity

3.1 Monitoring of nitrogen oxides emitted by take-off aircrafts

A monitoring campaign for relevant pollutants and meteorological parameters was held between 04.04.2011 – 11.04.2011, from an international airport perimeter. In-situ measurements were made using a mobile laboratory equipped with reference tools and meteorological station.

The results of measurement campaign were used as validation data for results obtained through NO_x pollutant dispersion modeling emitted from aircraft engines during take-off operation of the LTO cycle.

Since the release of nitrogen oxides NO_x reached the maximum at the highest thrust regime, by placing the monitoring system close to the runway, NO_x concentrations released by the aircraft take-off operation were highlighted.

To measure NO_x concentrations in the vicinity of the take-off/landing runway HORIBA APNA-360 equipment was used.

Meteorological parameters namely wind speed and direction, temperature and air pressure were also monitored. The location for measurement equipments inside the airport was chosen so as to identify the runway influence to the concentrations of monitored pollutants. The mobile system was placed near the runway, about 240 m from the runway center line, in accordance with measuring campaign purpose (Fig. 1). The dominant direction of the wind has been WSW – NW (Fig. 2).

Fig.1 The location of monitoring system of air pollutants and meteorological data

During this period, a radar based on ADS-B (Automatic Dependent Surveillance - Broadcast) technology to identify aircrafts which take-off was used. The engines types from the aircrafts were determined according to known data [14].

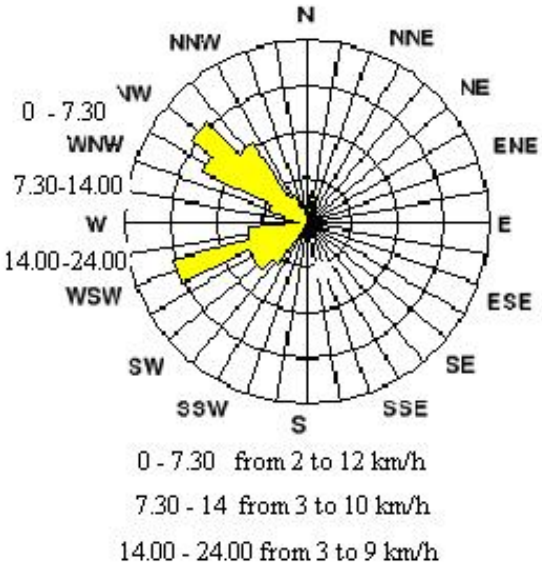

Fig.2 Wind direction and velocity values for analyzed time period

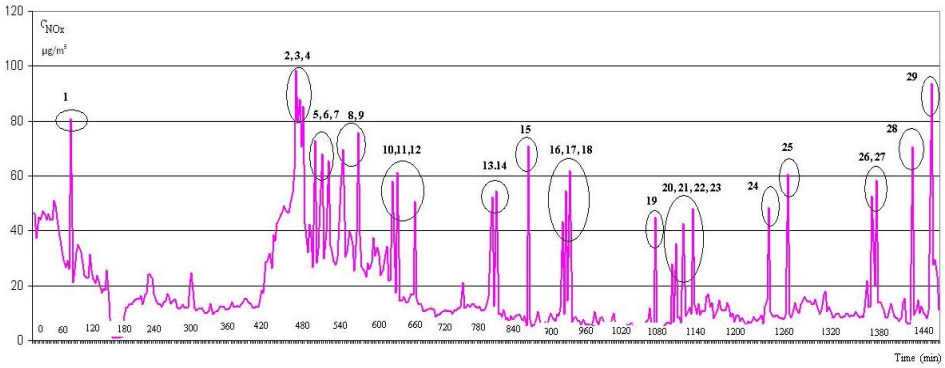

Fig.3 Dynamics of measured NO_x concentration at coordinates of monitoring system.

The analysis of data obtained during the development of experimental investigation, here given by mean of figure 3, revealed that these data, acquired on the day of 09.04.2011 provides the best information because in this day most take-offs occurred and wind blew from the runway towards the air pollution monitoring system.

It was found that during the approximately 24 hours (from 00:59 to 23:40), 29 aircrafts took off, namely: B 737-400 (9,17,19,20,28 in fig. 3), A 319-132 (6,11,12,18,25 in fig.3), A 319-112 (8,13,26 in fig.3), A 320-232 (1-5,7,10,14-17, 19-25, 27-29 in fig. 3)

Data measured for NO_x concentration, in receiver location, were correlated with data from ADS-B radar. The radar provided data about the time when some aircraft took off and the measured NO_x concentration was read in the same time. From fig 3 it is observed that the measured NO_x concentration varied for the 4 types of aircrafts, as follows: for B 737–400 B: 38 µg/m^3 ÷ 70.4 µg/m^3; for A 320–232: 42.5 µg/m^3 ÷ 98.6 µg/m^3; for A 319–132: 50.7 µg/m^3 ÷ 61.3 µg/m^3; for A 319–112: 61.7 µg/m^3 ÷ 69.82 µg/m^3. The height values correspond with the cases when we have very closed aircrafts departures (cases from figure 3: a) 2, 3 and 4; b) 5, 6 and 7; c) 13 and 14; d) 16, 17 and 18; e) 26 and 27). In these cases occurs an interaction of puffs from an aircraft which finish the take-of procedure with those generated from aircraft which begin the take-of procedure.

These measured values of NO_x concentrations are linked not only to emission sources, but to the speed and direction of the wind, which varied from time to time, during the whole period of the day.

3.2 NO_x pollutant dispersion modeling emitted from aircraft engines during take-off operation

The monitoring receiver is located at a distance of 240 m from the runway where NO_x concentration is measured after aircraft take-off, as shown in Fig. 4 [15].

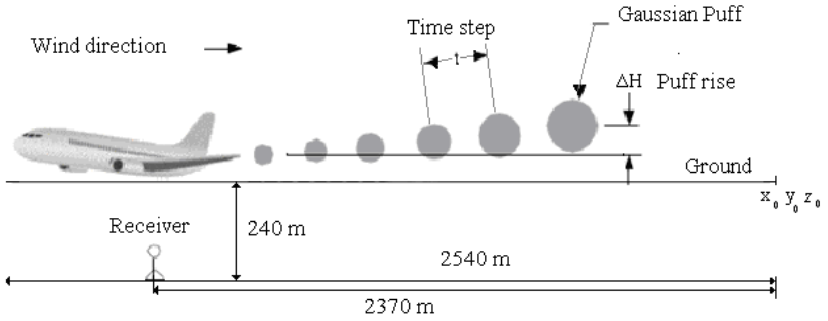

Fig.4 Input data for modeling NO_x concentration at the receiver

For modeling of NO_x pollutant dispersion emitted from aircraft engines during take-off operation, the quantity of NO_x emitted by each aircraft must be known. Starting from equation (19), the take-off NO_x emission is calculated, for each engine type of studied aircraft. We use that $\Delta m_{NOxk} = i_{NOxk} \times Q_{Dk}$ and $Q_{Dk} = \tau_k \times G_{mF\,k}$. Here for k=1 we have take-off flying stage. These data are presented in Table 1, where the numbers on green background, for each type of engine, were taken from ICAO Engine Emissions Data Bank (ICAO-EEDB) [16].

Table 1

Specific data to each engine type and specific to LTO cycle

Characteristic	Flight operation	ENGINE TYPE			
		CFM56-3B-2	IAE V2527-A5	IAE V2524-A5	CFM56-5B6/P
Time in mod, τ_k, s	k=1 Take-off	42			
	k=2 Climb out	132			
	k=3 Approach	240			
	k=4 Idle	1560			
NO_x emission index per mode, $i_{NOx,k}$, g/kg	k=1 Take-off	19.4	26.5	26.2	23.6
	k=2 Climb out	16.7	22.3	22	19.6
	k=3 Approach	8.7	8.9	9	9.2
	k=4 Idle	4.1	4.7	4.7	4
Fuel flow per mode, G_{mFk}, kg/s	k=1 Take-off	1.056	1.053	1.042	0.961
	k=2 Climb out	0.878	0.880	0.868	0.799
	k=3 Approach	0.314	0.319	0.328	0.275
	k=4 Idle	0.119	0.128	0.123	0.097
Consumed fuel/ flight	k=1 Take-off	44.352	44.226	43.764	40.362
	k=2 Climb out	115.896	116.16	114.576	105.468

mode, Q_{Dk}, kg	k=3 Approach	75.36	76.56	78.72	66
	k=4 Idle	185.64	199.68	191.88	151.32
Consumed fuel in LTO cycle, Q_{LTO}, kg (calculated)		421.248	436.626	428.94	363.15
Consumed fuel in LTO cycle, Q_{LTO} , kg (according to EEDB-ICAO)		421	437	429	363
NO_x emission for take-off operation, Δm_{NOx1} , g/engine		***860.4***	***1172.9***	***1146.6***	***952.5***

Gas flow speeds were calculated according to equation 4 for each engine type, depending on the specific technical characteristics ([17] – for Boeing 737-400 aircraft and [18] – for Airbus aircraft family (A 320-232, A 319-132, A 319-112)). The values are presented in Table 2.

Table 2

Speed gas jet calculation for aircrafts under study

Aircraft type	B 737-400	A 320-232	A 319-132	A 319-112
Engine type	CFM 56-3B-2	IAE V2527-A5	IAE V2524-A5	CFM56-5B6/P
Traction force Fn, Kgf	96.9	117.88	106.75	104.5
Traction force Fn, KN	988.050	12020.415	10885.471	10656.034
Inlet mass flow, G_m Kg/s	309.8	389.2	335	382.8
Aircraft speed v_a Km/h	871	871	871	871
Speed gas jet v_{ej} Km/h	902.895	901.885	903.494	898.837
Speed gas jet v_{ej} m/s	250.804	250.524	250.971	249.677

In Table 3 specific data for aircrafts and engines are presented, as well as measured data, which are used for modeling.

Table 3

Specific characteristics of aircrafts and monitoring system used in modeling

Type	Aircraft	B 737-400	A 320-232	A 319-132	A 319-112
	Engine	CFM 56-3B-2	IAE V2527-A5	IAE V2524-A5	CFM56-5B6/P
Technical specifications	Number of engines	2	2	2	2
	Take-off length, m	2540	2090	2164	2164
	Take-off speed, m/s	84.722	76.389	77.778	77.778
	T evacuated gases, K	1203.15	908.15	908.15	1223.15
	Evacuated gases speed, m/s	250.804	250.524	250.971	249.677

	Fan diameter, m	1.52	1.62	1.62	1.735
	Nozzle diameter, m	0.98	0.94	0.94	1.3
	Engine ground clearance, m	0.46	0.72	0.72	0.6
	Puff centre height z, m	1.22	1.53	1.53	1.4675
Receiver coordinates	x_r , m	2370	2370	2370	2370
	y_r, m	240	240	240	240
	z_r , m	3	3	3	3
Air temperature	Ta, °C	20	20	20	20
	Ta, [K]	293.15	293.15	293.15	293.15

The calculation follows to obtain F, ΔH and ΔH_f. We have the evacuated gases speed at the receiver, for B 737-400, as: $v_{e,r} = 84{,}772\ (2370/2540)^{1/2} = 81{,}838$ m/s and the revised evacuation speed for combustion gasses as: $v_{e,c} = 250{,}804 - 81{,}838 = 168{,}966$ m/s .

For B 737-400 aircraft it give F = 301,011 m^4/s^3; ΔH = 149,412 m; ΔH_f = 428,781 by replacing of computed values in equations 2, 3 and 6. Table 4 concentrates these calculations (F, ΔH and ΔHf) for all aircrafts under study when their departures occur without interactions.

Table 4

Values for F, ΔH and ΔH_f calculated for non interacted aircrafts departures

Type	Aircraft	**B 737-400** (9 in fig. 1)	**A 320-232** (15 in fig.1)	**A 319-132** (8 in fig.1)	**A 319-112** (25 in fig.1)
	Engine	**CFM 56-3B-2**	**IAE V2527-A5**	**IAE V2524-A5**	**CFM56-5B6/P**
Buoyancy flow calculation	(revised) speed of the gas ($v_{e,c}$), [m/s]	168.966	169.179	169.575	168.281
	The speed at receiver level [m/s]	81.838	81.345	81.396	81.396
	Buoyancy flow (F), [m^4/s^4]	301.011	248.272	248.854	530.316
Calculation of (u_z) at the puff center height	Reference height (z_r), m	10	10	10	10
	Wind speed at 10m (u_r), [m/s]	3.8	3.8	3.8	3.8
	Power coefficient (p)	0.15	0.15	0.15	0.15
	Wind speed at the puff centre height (u_z), [m/s]	2.772	2.867	2.867	2.850
Puff rise height	At distance x (ΔH), [m]	149.412	135.441	135.546	175.524
	Final rise (ΔH_f), [m]	428.781	369.226	369.745	585.833

Now are calculated the dispersion parameters σ_x, σ_y and σ_z, which are required by the basic relation of the puff model. For D stability class, which is indicated by our meteorological measurements, we have, respect to relations (13) and (14), a = 8.3333, b = 0.72382, c = 32.093 and d = 0.6443. For r, as it is

derived from figure 4, we consider the value r = 2.37 km. The σ_x, σ_y and σ_z computation is concentrated by table 5.

Table 5

Calculated dispersion parameters for non interacted aircrafts departures

Type	Aircraft	B 737-400 (9 in fig. 1)	A 320-232 (15 in fig.1)	A 319-132 (8 in fig.1)	A 319-112 (25 in fig.1)
	Engine	CFM 56-3B-2	IAE V2527-A5	IAE V2524-A5	CFM56-5B6/P
Dispersion coefficients calculus (σ_x, σ_y, σ_z) and the mixture height (H_m)	$\sigma_{xt} = \sigma_{yt}$, m	149.211	149.211	149.211	149.211
	σ_{zt} , m	55.958	55.958	55.958	55.958
	$\sigma_{xr} = \sigma_{yr} = \sigma_{zr}$, m	42.689	38.697	38.728	50.150
	σ_x , m	155.198	154.148	154.155	157.413
	σ_y , m	155.198	154.148	154.155	157.413
	σ_z , m	70.382	68.035	68.052	75.142
	H_m, m	150.632	136.971	137.076	176.991

Then all the obtained values are replaced in equation 1 which can be write as $c = A \times B \times C \times (D + E + F)$. Here: $A = \dfrac{\Delta M}{(2\pi)^{3/2}\sigma_x\sigma_y\sigma_z}$, $B = \exp\left[-\dfrac{1}{2}\left(\dfrac{x_p - x_r}{\sigma_x}\right)^2\right]$,

$C = \exp\left[-\dfrac{1}{2}\left(\dfrac{y_p - y_r}{\sigma_y}\right)^2\right]$, $D = \exp\left[-\dfrac{1}{2}\left(\dfrac{z_p - z_r}{\sigma_z}\right)^2\right]$, $E = \exp\left[-\dfrac{1}{2}\left(\dfrac{z_p + z_r}{\sigma_z}\right)\right]$,

$F = \exp\left[-\dfrac{1}{2}\left(\dfrac{2H_m - z_p - z_r}{\sigma_z}\right)^2\right]$ and $c = c_{NO_x} = c_{NO_X}(x_r, y_r, z_r)$

Table 6 contain the results obtained after modeling of NO_x pollutant dispersion, emitted during aircrafts take-off operations which are considered in the above tables.

Table 6

NOx concentration at the receiver for non interacted aircrafts departures

Type	Aircraft	B 737-400 (9 in fig. 1)	A 320-232 (15 in fig.1)	A 319-132 (8 in fig.1)	A 319-112 (25 in fig.1)
	Engine	CFM 56-3B-2	IAE V2527-A5	IAE V2524-A5	CFM56-5B6/P
Terms of modeling equation	A	3.22105E-05	4.60313E-05	4.50336E-05	3.24983E-05
	B	0.548852498	0.544369126	0.5444017	0.558133994
	C	0.302492328	0.29758751	0.297623001	0.312773266
	D	0.999680245	0.999766606	0.999766724	0.999791911
	E	0.998204104	0.997785782	0.997786899	0.998234541
	F	0.000135565	0.000393517	0.000390247	2.00384E-05

	Engine gen., [μg/m^3]	10.6848	14.8985	14.5783	11.3353
	Aircraft gen., [μg/m^3]	**21.3696**	**29.7972**	**29.1565**	**22.6707**

The concentrations reported within table 6 must be corrected taking into account the NO_x concentration level before aircraft take-off. So to each computed value will be added the NO_x concentration before aircraft departure (31 μg/m^{3}for the fly number 8 (fig.1), 28 μg/m^{3}for the fly number 9, 10 μg/m^{3}for the fly number 15 and 13 μg/m^{3}for the fly number 25). For the cases where we have interaction between aircrafts departures the same rule has been used. Figure 5 contains a comparison between measured and computed c_{NO_x} concentration values. Supplementary here has given the c_{NO_x} background concentration values because they show the correction given to the computed values and also they characterize, as mean, the pollution dynamics inside of airport area.

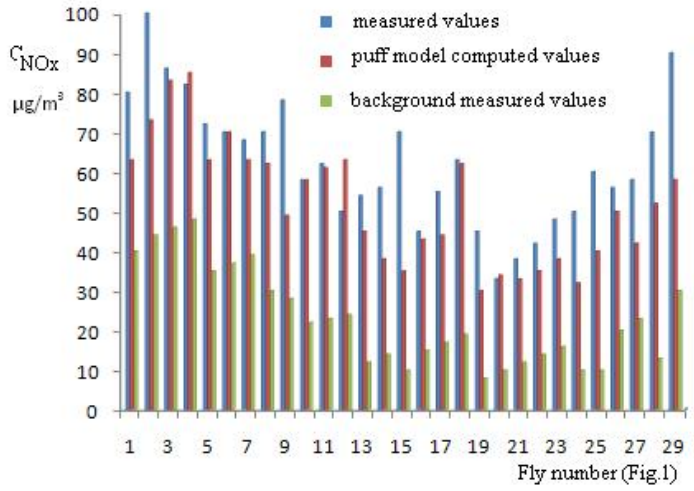

Fig.5 Measured and computed values for all investigated aircrafts departures

From figure 5 it is observed that the modeling obtained values of NO_x concentration relative to each aircraft departure are in good accord for 7 aircrafts departures. For remainder 22 departures the computed values are lower than the values measured in the same location. It is normal to be so, because our computation has been based on catalog data concerning the aircrafts engines. In exploitation an aircraft engine change it basic fuel consumption and also the fuel burning quality. An increasing with 10-15 % of $G_{mF,k}$ in table 1 increase the c_{NO_x} computed values, of above mentioned 22 departures, to a level concordant

with c_{NO_x} measured values. The same effect is obtained by an increasing in table 1, with a 10-15 %, of $i_{NOx,k}$ index. The LTO cycle aircraft out operation can be another motif of differences between measured and computed c_{NO_x} concentrations. Figure 5 sustain that the use of puff model for estimation of atmospheric dispersion of pollutants generated by an aircraft in LTO cycle is a good option. The background measured values show that in airport area are fixed and mobile sources of emissions with variable time activity. They also sustain that our system measures local pollution of the entire area under analysis. Considering the eject gas composition from an aircraft engines, the puff model can compute the atmospheric dispersion of all generated pollutants.

4. Conclusions

The advantages of modeling are the rapid results obtained, low costs and that it can be applied to various scenarios related to the operation types and sources of pollution.

Even if for the same type of aircraft may exist variations during actual operation, the use of a fixed LTO cycle provides a constant reference frame through which can be compared the aircraft engines performance in terms of emissions.

Considering that the distribution of NOx concentration is dependent on weather conditions more than the variation emissions, for dispersion modeling, meteorological data accuracy may be more important than the complexity of emissions calculations [19].

The original aspects of this paper are related to:

- the use of puff model for characterization of NO_x dispersion from an aircraft in LTO cycle;
- the development of a computation algorithm for puff model application to an concrete case;
- identifying of an aircraft in LTO cycle using virtual radar based on ADS-B technology and use of data in the modeling algorithm;
- settlement of a procedure to use the mobile station for collection of meteorological data and for analyzing air pollution caused by aircraft, as pollutants mobile source in the airport area;
- using measured values to validate results obtained by modeling;
- possibility to extend the modeling for other pollutants emitted by aircrafts, for all LTO cycle operations, as well as for other types of aircraft, in order to set up a database. It may be accessed both by airport authorities and environmental authorities that control the amount of emissions produced by sources of pollution in the airport area.

Acknowledgements:

This work was supported by project nr.1306P/2010 between COMOTI Romania and a Romanian airport. For participation to experimental research and data analysis we address thanks to Environment Team from COMOTI Romania. Thanks also to Romanian airport where our measurements has been developed.

R E F E R E N C E S

[1] *G.Ratliff, C.Sequeira, I.Waitz, M.Ohsfeldt, Th.Thrasher, M.Graham, T.Thompson*, Aircraft Impacts on Local and Regional Air Quality in the United States, PARTNER Project 15 final report, October 2009
[2] *** International Civil Aviation Organization, Doc 9889, Airport Air Quality Manual, 2011
[3] *G.Adamkiewicz, H-H.Hsu, J.Vallarino, S.Melly, J.Spengler, J.Levy,* Nitrogen dioxide concentrations in neighborhoods adjacent to a commercial airport:a land use regression modeling study, Environmental Health, November 2010
[4] ***DIRECTIVE 2008/50/EC OF THE EUROPEAN PARLIAMENT AND OF THE COUNCIL on ambient air quality and cleaner air for Europe, May 2008
[5] *O.I Zaporozhets, K.V Synylo*, Monitoring and Modelling of Air Pollution Produced by Aircraft Engine Emission Inside the Athens International Airport, Environmental Protection, NAU Proceedings, vol 4, 2009, pp. 59-64
[6] *D. C.Carlslaw, S.D.Beevers, K.Ropkins, M.C.Bell*, Detecting and quantifying aircraft and other on-airport contribution to ambient nitrogen oxides in the vicinity of a large international airport, Atmospheric Environment, vol.40, April 2006, pp. 5424-5434
[7] *Brian Y. Kim,* Predicting Air Quality Near Roadway Intersections Through the Application of a Gaussian Puff Model to Moving Sources, PhD Thesis, University of Central Florida Orlando, 2004
[8] *Briggs, G.A*., Discussion on Chimney Plumes in Neutral and Stable Surroundings, Atmospheric Environment, vol.6, pp 507-510, 1972.
[9] *C. Riegler, C. Bichlmaier,* The geared turbofan technology - Opportunities, challenges and readiness status, 1st CEAS European Air and Space Conference, Berlin, Germany 10–13 September 2007
[10] *Maria, G.,* Evaluarea cantitativa a riscului proceselor chimice si modelarea consecintelor accidentelor,Ed. Printech, Bucharest, 2007
[11] *Turner, D. Bruce*, Workbook of Atmospheric Dispersion Estimates, An Introduction to Dispersion Modeling, Second Edition, CRC Press, Inc., 1994
[12] Pasquill, F. Atmospheric dispersion of pollution, Journal of the Royal Meteorological Society, vol. 97, pp 369-395, 1971.
[13] *** Recommendation ECAC/27-4, NOx Emission Classification Scheme, July 2003
[14] *** Gatwick Aviation Society http://www.gatwickaviationsociety.org.uk/modeslookup.asp
[15] *Ben H. Sharp*, A New Simulation Model, Annual UC Symposium on Aviation Noise and Air Quality, March, 2008
[16] *** http://easa.europa.eu/environment/edb/aircraft-engine-emissions.php
[17] *** http://www.b737.org.uk/techspecsdetailed.htm
[18] *** http://en.wikipedia.org/wiki/Airbus_A320_family
[19] *Emanuel Fleuti, Silvio Maraini, Ulf Janicke*, Air Quality Assessment Sensitivities–Zurich Airport Case Study**,** Unique/ Swiss, 2009